



Research Paper

Tracking nanoplastics in freshwater microcosms and their impacts to aquatic organisms



Miguel Tamayo-Belda^a, Ana Villanueva Pérez-Olivares^a, Gerardo Pulido-Reyes^{b,c}, Keila Martin-Betancor^a, Miguel González-Pleiter^a, Francisco Leganés^a, Denise M. Mitrano^d, Roberto Rosal^e, Francisca Fernández-Piñas^{a,*}

^a Department of Biology, Faculty of Science, Universidad Autónoma de Madrid, E-28049 Madrid, Spain

^b Eawag, Swiss Federal Institute of Aquatic Science and Technology, Ueberlandstrasse 133, 8600 Dübendorf, Switzerland

^c Department of Environment and Agronomy, Spanish National Institute for Agricultural and Food Research and Technology (INIA-CSIC), Crta. de la Coruña, km 7.5, 28040 Madrid, Spain

^d Environmental Systems Science Department, ETH Zurich, 8092 Zurich, Switzerland

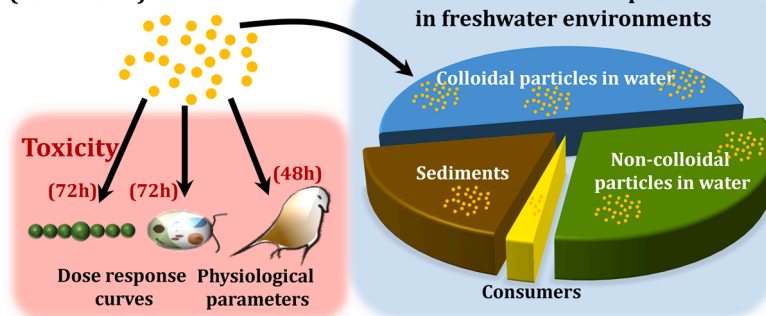
^e Department of Chemical Engineering, Universidad de Alcalá, E-28871 Alcalá de Henares, Madrid, Spain

HIGHLIGHTS

- Pd-doped polystyrene nanoplastics were only lethal at high concentrations.
- EC₅₀s ranged from 49 mg NPLs/L for *D. magna* to 248 mg NPLs/L for *C. reinhardtii*.
- Pd-doped nanoplastics caused membrane damage by physical interaction.
- After 48 h ~ 50 % of the nanoplastics remained in water under colloidal stability.
- The presence of organisms promoted nanoplastic settlement in the sediments.

GRAPHICAL ABSTRACT

Pd-doped nanoplastics (286 ± 4 nm)



ARTICLE INFO

Editor: Dr. R Teresa

Keywords:

Aquatic organisms
Environmental fate
Freshwater microcosms
Nanoplastics
Toxicity

ABSTRACT

In this work, we used palladium-doped polystyrene NPLs (PS-NPLs with a primary size of 286 ± 4 nm) with an irregular surface morphology which allowed for particle tracking and evaluation of their toxicity on two primary producers (cyanobacterium, *Anabaena* sp. PCC7120 and green algae, *Chlamydomonas reinhardtii*) and one primary consumer (crustacean, *Daphnia magna*). The concentration range for *Anabaena* and *C. reinhardtii* was from 0.01 to 1000 mg/L and for *D. magna*, the range was from 7.5 to 120 mg/L. EC₅₀s ranged from 49 mg NPLs/L for *D. magna* (48hEC₅₀s) to 248 mg NPLs/L (72hEC₅₀s for *C. reinhardtii*). PS-NPLs induced dose-dependent reactive oxygen species overproduction, membrane damage and metabolic alterations. To shed light on the environmental fate of PS-NPLs, the short-term distribution of PS-NPLs under static (using lake water and sediments) and stirring (using river water and sediments) conditions was studied at laboratory scale. The results showed that

* Corresponding author.

E-mail address: francisca.pina@uam.es (F. Fernández-Piñas).

most NPLs remained in the water column over the course of 48 h. The maximum percentage of settled particles (~ 30 %) was found under stirring conditions in comparison with the ~ 10 % observed under static ones. Natural organic matter increased the stability of the NPLs under colloidal state while organisms favored their settlement. This study expands the current knowledge of the biological effects and fate of NPLs in freshwater environments.

1. Introduction

The incorporation of nanoplastics (NPLs, < 1 μm) in daily used products, along with fragmentation of the large amount of plastic litter into secondary micro (MPs, < 5 mm) and nanoplastics, are increasing the concern regarding their distribution and toxicity in freshwater environments [19,21,25,39,63]. In particular, NPLs may behave as stable colloids thereby increasing the dissemination of plastic fragments in the environment [38,69,71]. Their fate and distribution have been studied by modeling their behavior throughout different environments considering different polymer types and size ranges [31], and by microcosm experiments using metal-doped NPLs [20]. Despite those recent studies, the distribution of NPLs in the environment remains scarcely studied in multi-component systems.

The use of techniques focused on the identification and analysis of NPLs, such as pyrolysis-gas chromatography-mass spectrometry (Py-GC-MS), have gained increasing attention during the last years aiming at solving the challenges of detecting and analyzing NPLs in complex matrices and biological samples [3,5,64,74]. However, these techniques are time-consuming and not as applicable for NPLs as they are for larger sized MPs particles for which they have primarily been used to date. A novel approach based on the synthesis of metal-doped NPLs, (basically, Pd and Al), which can be easily tracked by techniques appropriate for trace metals analysis, such as ICP-MS, has been recently developed [40, 67] and has proven suitable in different studies to assess the fate and biological uptake of NPLs. Pd-doped NPLs were used to assess the fate through different water systems (waste water and drinking water treatment plants [16,27,48], to environmental fate in freshwater simulated conditions [20], uptake into both freshwater and terrestrial organisms [22,50,9] and evaluation of the uptake and distribution of NPLs in plants [49].

Toxicological studies using primary producers have reported different effects of NPLs at concentrations in the low mg/L range, including photosynthesis impairment, shifts in intracellular pH, increase in reactive oxygen species (ROS) which may lead to oxidative stress, membrane damage and alterations in gene and protein expression [6,16, 31,66,69]. In this regard, cyanobacteria and microalgae such as *Anabaena* sp. PCC7120 and *Chlamydomonas reinhardtii* have been widely used for nanotoxicological studies given their widespread distribution and their environmental relevance as base of the trophic chain [19,47, 61,66]. For primary and secondary consumers, reported effects induced by NPLs include mortality, body internalization and dissemination, intergenerational alterations, bioaccumulation and changes in genetic expression, among others [11,36,38,55,58]. However, most studies to date have focused on commercially available, spherical polystyrene NPLs (PS-NPLs) with a smooth surface morphology, potentially overlooking the true impact of more realistic NPLs which usually display irregular shapes and comparatively rougher surface morphologies [12, 68]. For instance, in primary human monocytes and monocyte derived dendritic cells, irregular PS-NPLs induced a significantly higher pro-inflammatory response compared to spherical PS-NPLs [70]. In this regard, there is a lack of knowledge regarding the toxicological behavior of NPLs of different shapes and particle chemistries.

In this work, the environmental impact of metal (Pd)-doped PS-NPLs with a rough surface morphology was evaluated using three ecologically relevant freshwater organisms: the filamentous cyanobacterium *Anabaena* sp. PCC7120 and the green alga *Chlamydomonas reinhardtii* Dangeard (strain CCAP 11/32A mt⁺) were chosen as representative photosynthetic organisms since they play a key role as primary

producers in freshwater environments. The small crustacean *Daphnia magna*, a primary consumer and a particle-ingesting organism that is widespread in freshwater ecosystems, was also included in the toxicological assessment. The effects of PS-NPLs on the physiology and structure of the organisms, as well as their potential internalization were assessed. Metal (Pd)-doped PS-NPLs allowed tracking their environmental distribution in the different freshwater environmental compartments (water column, sediment, biota). Natural water and sediment were collected from a lake and a stream and the primary producer *Chlamydomonas reinhardtii* and the consumer *Daphnia magna* were used in microcosm studies (under static and stirring conditions). Principal component analysis (PCA) was used to weigh the role of different physicochemical and biological parameters in the environmental fate of the PS-NPLs. The systematic study of NPLs fate in environmentally relevant matrices and test conditions will help in the understanding of the distribution and toxicity of NPLs across different environmental compartments.

2. Materials and methods

2.1. Metal-doped nanoplastics and chemicals

Polyacrylonitrile-core polystyrene-shell nanoplastics (PS-NPLs) were synthesized as previously described by Mitrano et al. [40]. Briefly, NPLs consisting of a polyacrylonitrile core with Pd doping and PS shell were made, with a final Pd content of approximately 0.3 w/w. The outer PS surface had a rough surface morphology and the leaching of the metal from these NPLs has previously been proven to be negligible in a variety of environmental and biological test conditions [49,40,48]. This means that 1) the Pd can act as a conservative tracer to track NPs and 2) no metal leaching would confound toxicological results. To quantify the amount of unreacted organic compounds coming from the synthesis of PS-NPLs (e.g. released oligomers, organic surfactants or unreacted monomers), 20 mL suspensions were filtered through previously washed ultracentrifugation tubes with 50 kDa MWCO filters (Vivaspin 20, Sartorius AG) to calculate the concentration of non-particulate organic material by means of total organic carbon (TOC) measurements using a Shimadzu TOC-VCSH analyzer equipped with an ASI-V autosampler. The carbon concentration in the filtered sample indicated an amount of soluble organic matter of 1.42 ± 0.02 %.

The mass concentration of the stock PS-NPLs suspension was assessed by TOC measurements as previously described by González-Pleiter et al., [19]. For ICP-MS measurements, samples were subjected to HNO₃ acid digestion using a microwave oven UltraWAVE (Milestone). Subsequently, the Pd concentration was measured by ICP-MS NexION 300XX (Perkin-Elmer) as described elsewhere [48]. According to the nominal concentration, the stock suspension of PS-NPLs was 66.01 mg/mL with Pd/PS-NPLs ratio of approximately 3.5 $\mu\text{g}/\text{mg}$ (Table S1). Particle size distribution was determined using a concentration of 50 mg/L in ultra-pure water at 25 °C by dynamic light scattering (DLS). Transmission electron microscopy (TEM) was used to confirm particle size and morphology using a 100 mg/L suspension stained with 2 % uranyl acetate by means of a JEOL (JEM 1400) electron microscope (100 kV). According to the nominal size, based on intensity distribution, PS-NPLs displayed a peak of 286 ± 4 nm and revealed few aggregates around 1 μm that were negligible as revealed by the TEM analysis. The results for the main parameters studied are shown in Fig. S1. Surface net charge of the PS-NPLs was measured using a concentration of 50 mg/L in ultra-pure water at 25 °C and pH 7 by electrophoretic light scattering

(ELS). PS-NPLs stock suspension showed a strongly negative ζ -potential of -41.8 ± 0.4 mV, at pH 7, indicating a stable colloidal suspension. Additionally, the particle number concentration was quantified in serial stock dilutions in ultra-pure water by Non-Invasive Back-Scatter optics (NIBS®) and Multi-Angle Dynamic Light Scattering (MADLS®) at 25 °C using a Zetasizer Ultra (Malvern Panalitical). Measurements were carried out by triplicate.

In order to study the toxic mechanism of PS-NPLs, seven fluorescent probes, specific for different physiological parameters, were obtained from Thermo Fisher: 2',7'-dichlorodihydrofluorescein diacetate, dihydrorhodamine 123, dihydroethidium, Bis-(1,3-dibutylbarbituric acid) trimethine oxonol, propidium iodide, 2',7'-bis(2-carboxyethyl)-5(6)-carboxy fluorescein and fluorescein diacetate. Specific information, concentration and incubation time are described in Table S2. Propidium iodide was prepared in ultra-pure water and stored at 4 °C while all the other fluorochrome stock solutions were prepared in dimethyl sulfoxide and stored at -20 °C prior to use.

2.2. Bioassays

Anabaena sp. PCC7120 (hereinafter *Anabaena*) and *Chlamydomonas reinhardtii* Dangeard (strain CCAP 11/32A mt+; hereinafter, *C. reinhardtii*) were routinely grown at 28 °C at a light intensity of ~ 65 μ E on a rotary shaker in 250 mL Erlenmeyer flasks with 100 mL of AA/8 + N (8-fold dilution of Allen & Arnon medium supplemented with 5 mM of nitrate, Table S3) and TAP/6 (6-fold dilution of TAP medium, Table S4), respectively. Cells were washed three times before each assay. Exposure experiments were carried out in triplicate with 10 mL of the corresponding culture medium in 25 mL Erlenmeyer flasks for 72 h [41] with minor modifications. The impact of increasing exposure concentrations of PS-NPLs (0.1, 1, 10, 100, 200, 500, 700 and 1000 mg/L) on both organisms was assayed by triplicate, non-exposed cells were used as controls. Cell growth was assessed spectrophotometrically at 750 nm. Dry weight was determined by using growth curves (*Anabaena* dry weight was determined as described by Tamayo-Belda et al. [62] and for *C. reinhardtii* using the growth curve shown in Fig. S2). The potential interference of PS-NPLs suspensions was assessed by measuring and subtracting the contribution of NPLs suspensions alone to the turbidity at the same optical density used for the dry weight calculations. Acute immobilization bioassays with *Daphnia magna* (hereinafter *D. magna*) were conducted using a commercial test kit (Daphtoxkit FTM, Micro-BioTests Inc., Ghent, Belgium). *D. magna* neonates (less than 24 h after hatching) were exposed to increasing concentrations of PS-NPLs: 0 (control), 7.5, 15, 30, 60 and 120 mg/L. The bioassays with *D. magna* neonates were conducted according to the Standard Operational Procedures of Daphtoxkit FTM adding 5 neonates by test well (4 by exposure concentration) for 48 h in the darkness at 20 °C. The final exposure concentrations for *Anabaena*, *C. reinhardtii* and *D. magna* were chosen based on previous range-finding tests with these same nanoparticles and other nanoparticles in a variety of organisms [17,57,60] and following the OECD Test Guidelines 201 and 202 [41,42]. The dose response curves of the photosynthetic organisms and *D. magna* were determined after an exposure time of 72 and 48 h, respectively. The effective concentrations of the PS-NPLs that caused 10 %, 50 % and 80 % (EC_{10} , EC_{50} , EC_{80}) of growth inhibition for *Anabaena* and *C. reinhardtii* and immobilization for *D. magna* were calculated using the drc package of RStudio software (Version 1.4.1717).

2.2.1. Analysis of mechanisms of toxic action

To study the mechanism of toxic action of PS-NPLs, the three organisms were exposed to two concentrations: one lower than each EC_{10} value and a sub-lethal one close to each EC_{50} value. The physiological study was assessed by fluorimetry and fluorescence microscopy depending on the organism. *Anabaena* and *C. reinhardtii* were exposed to 10 and 200 mg PS-NPLs/L. After 72 h, samples were analyzed in a microplate reader Fluoroskan Ascent® fluorometer (Thermo Fisher

Scientific) with an excitation laser at 488 nm and four detectors corresponding to four wavelength range channels: 505–550 (FL1), 550–600 (FL2), 600–645 (FL3) and > 645 (FL4). Seven fluorescent probes were applied to evaluate five physiological parameters: ROS level, membrane potential, membrane integrity, intracellular pH and metabolic activity. The concentration and incubation time used for each fluorescent probe can be found in Table S1, and further details are available elsewhere [19, 36,62]. Autofluorescence from chlorophylls *a* and *b* was subtracted when there was an overlap with the probe emission. A volume of 180 μ L of culture aliquots was placed in a 96-well plate wells. Then, 20 μ L of the corresponding fluorochrome was added and after the appropriate incubation time, the plates were analyzed by fluorimetry using two replicates by treatment. Four measurements were carried out for each plate. Results were expressed as percentage with respect to the control (non-exposed cells). *D. magna* neonates were also exposed to low (below EC_{10}) and a high (close to EC_{50}) sublethal concentration: 10 and 80 mg/L of PS-NPLs for 48 h. Then, 4 neonates were collected and individually incubated in 200 μ L of the corresponding probe at room temperature and in darkness. Seven fluorescent probes were used to assess the status of five physiological parameters: ROS level, membrane potential, membrane integrity, intracellular pH and metabolic activity. After incubation, the solution containing the probe was removed and the neonates were carefully transferred to glass slides in 10 μ L of fresh medium (FW, Daphtoxkit) to be analyzed by fluorescence microscopy. Unexposed organisms (controls) followed the same procedure, and no toxicity was observed due to the incubation with the fluorescent probes [19].

2.2.2. Transmission electron microscopy/Energy dispersive X-Ray analysis (TEM/EDX)

TEM analysis was conducted to study the physical interaction between organisms and PS-NPLs as well as to evaluate potential internalization and alterations of the cells after NPL exposure. The biomass from aliquots of 2 mL of *Anabaena* and *C. reinhardtii* exposed to the highest concentration of PS-NPLs was collected by centrifugation at 10,000 rpm and the supernatant was discarded. In the case of *D. magna*, three neonates were collected by treatment and the excess of media was carefully removed by pipetting. *Anabaena*, *C. reinhardtii* and *D. magna* were immersed in 1 % glutaraldehyde plus 4 % formaldehyde in sodium cacodylate buffer (0.1 M) at pH 7.3 during 24 h at 4 °C. Then, cells and neonates were fixed in agar blocks in 2.5% glutaraldehyde in sodium cacodylate buffer (50 mM) with $CaCl_2$ (5 mM) for 1.5 h at 4 °C. Post-fixation was performed in osmium tetroxide in phosphate buffer for 2 h at 4 °C. Section of the samples were obtained by a Leica Reichert Ultracut S ultramicrotome and stained with 2 % uranyl acetate. Images were taken with a JEOL 1400 electron microscope (100 kV), coupled with EDX to track the presence of Pd from NPLs in treated samples.

2.3. Environmental fate assay: microcosms study

The goal of the environmental fate assay was to elucidate the short-term PS-NPLs distribution between four different environmental compartments including: i and ii) NPLs in the water column, divided by filtration into particles in colloidal state (< 1 μ m) versus non-colloidal state (> 1 μ m), iii) in the sediments and iv) in *Daphnia magna*, performed in microcosms experiments under static and stirring conditions (Fig. 1). Water and sediment samples were collected from the Pinilla reservoir (40°56'56.5"N 3°46'52.6"W) in Madrid (Spain) and used for the static assay. For the stirring assay, water and sediment were collected from a nearby stream of the same reservoir (40°56'52.6"N 3°47'22.0"W). Approximately, 5 L of water and 5 kg of sediments were collected from each location in glass bottles and aluminum boxes, respectively, and immediately transported to the laboratory. Both sample types were sterilized by autoclave and were kept at 4 °C until use. Microcosms assays were conducted in 25 mL glass beakers under static conditions, for the static assay, and dynamic conditions by using

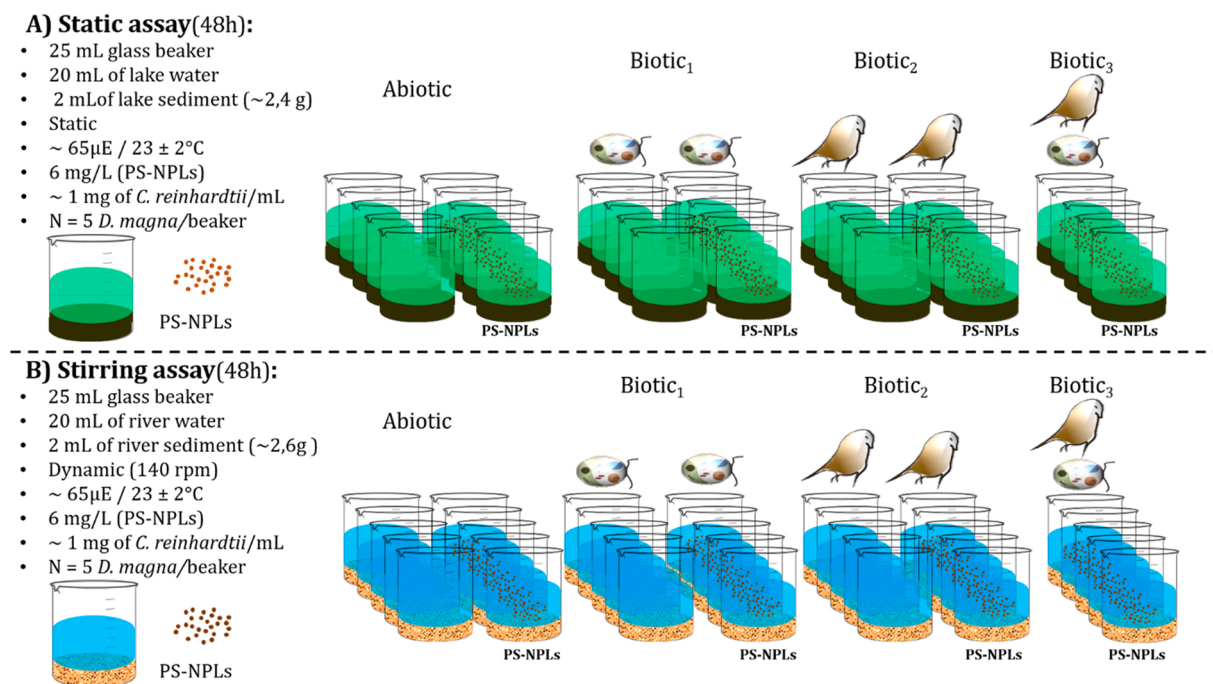


Fig. 1. Experimental design for the environmental fate assay for static (A) and stirring (B) microcosms experiments. Four different treatments were assayed for each condition (static/stirring), from left to right: Abiotic (water + sediment + PS-NPLs); Biotic₁ (water + sediment + *C. reinhardtii* + PS-NPLs); Biotic₂ (water + sediment + *D. magna* + PS-NPLs); Biotic₃ (water + sediment + *C. reinhardtii* + *D. magna* + PS-NPLs). Abiotic controls of waters without PS-NPLs and growth and survival controls of organisms without PS-NPLs were also assessed.

an orbital shaker at 140 rpm for the stirring assay. In order to decrease the complexity of the study, the fate assays were conducted with two of the three organisms used for the toxicological study. Thus, *C. reinhardtii* was selected as phototrophic organism as this organism is able to actively move by flagella within the water column and over the sediment. In addition, this organism is a typical food source for *Daphnia magna*. To address the role of primary consumers, *D. magna* was selected since it is capable of randomly distributing between the water column and around the surface of the sediments as well as able to actively ingest *C. reinhardtii* for feeding.

The procedure for both conditions (static and stirring assays) were carried out as follows: First, the sediments (~ 2.4 and ~ 2.7 g of sediments from lake and river, respectively, were added in each beaker to ensure similar sediment depth in both systems) and then, the corresponding water (20 mL) were added to the sterilized 25 mL glass beakers on top of the sediments. In order to avoid turbidity coming from the sediments after water addition, the beakers were left 24 h under sterile and static conditions before starting the experiments. A fresh working stock suspension of PS-NPLs was prepared to ensure an initial size distribution lower than 1 μ m. Accordingly, the original stock was diluted and filtered (GF/B; < 1 μ m) to obtain a suspension that was newly characterized in terms of PS-NPLs and Pd concentration (600 mg NPL/L and 2.14 mg Pd/L, respectively). After allowing the suspension to settle, aliquots of PS-NPLs were added at a final concentration of 6 mg NPLs/L (the concentration where no observable effects on the organisms were observed from the toxicological study). Next, *C. reinhardtii* cells (routinely growing as described above) were washed and added into the corresponding treatments to reach an initial concentration of ~ 1 mg (dry weight)/mL (using the growth curve shown in Fig. S2). *D. magna* was grown for 10 days at 25 \pm 1 $^{\circ}$ C with a 16 h/8 h light dark period and fed with 1 mg of *C. reinhardtii* per day. Five organisms were added per replicate. The same algal cellular concentration and number of *D. magna* were inoculated for the treatment in which both organisms were simultaneously present. Finally, the beakers were covered with aluminum foil (perforated and sterilized) and randomly distributed before running the assay.

2.3.1. Pd-doped NPLs tracking analysis

Material retained by the filters, waters, sediments and *D. magna* individuals were chosen as the four main compartments to study the distribution of PS-NPLs in the environmental compartments depicted in Fig. 1. These four compartments, schematized in Fig. S3, were: (i) NPLs dispersed or in particulate material less than 1 μ m suspended as a colloid within the water column, denoted as “colloidal water compartment”, hereafter cWC (this compartment refers to particulate material that was able pass the cut-off and to be established as colloids by IUPAC [24] (ii); NPLs in particulate material higher than 1 μ m suspended in the water column denoted as “non-colloidal water compartment”, hereafter ncWC (this compartment refers to particulate material that was not able to pass the pore size of the filter); (iii) NPLs adhered to the sediment which was denoted as “sediment compartment”, hereafter SC; and (iv) NPLs in the individuals of *D. magna*, hereafter, DC.

After 48 h exposure, aliquots in each environmental compartment were sampled to evaluate several biological and physicochemical parameters. NPLs were tracked by measuring Pd concentrations in each compartment by ICP-MS. Water was carefully transferred into new glass beakers without disturbing the sediment layer. This supernatant was homogenized and filtered through a GF/B filter with a pore size of 1 μ m to isolate the material within the colloidal size range (material below 1 μ m as defined by IUPAC [24] from larger particles. Both water and filters were stored at – 80 $^{\circ}$ C until further analysis. Sediments were dried in the same beakers used for ecotoxicological assays for 72 h at 40 $^{\circ}$ C. Subsequently, sediments were transferred to sterilized tubes and stored at – 80 $^{\circ}$ C until further analysis. A schematic representation of the sampling and measurement methodology can be found in Fig. S4. Filters (ncWC), waters (cWC), sediments (SC), and *D. magna* neonates (DC) were acid-digested and the NPLs in each compartment were tracked by measuring Pd concentrations as a proxy for the NPLs.

2.3.2. Analysis of factors involved in NPLs distribution

For water and filter samples, the extraction of chlorophyll *a* and *b* from *C. reinhardtii* was performed in acetone (90 %) for 24 h at 4 $^{\circ}$ C in the dark and were determined by spectrophotometry (664 and 647 nm)

as described by Ahmed [11]. For sediment samples, chlorophyll extraction was performed in 90 % acetone by thoroughly vortexing for 15 s followed by 15 s of ultrasonication. This procedure was repeated before incubating the samples for 24 h at 4 °C in the dark (adapted from Cirés et al. [8]). Water chemistry (pH, conductivity and organic matter quantified by TOC using a Shimadzu TOC-VCSH analyzer), sediment moisture (measured by comparing the weight before and after drying them for 3 days at 60 °C), hydrodynamic size distribution (assessed by DLS using a Zetasizer Nano, Malvern Instruments) and ζ -potential (assessed by ELS using a Zetasizer Nano) of the filtered water were also assessed.

2.4. Quality assurance/quality control (QA/QC)

Glass beakers were washed with ultra-pure water, covered with aluminum foil, and sterilized before performing the environmental fate assay. The preparation of the assay was conducted under sterilized conditions in a flow cabinet. The background concentrations of Pd in the waters, sediments and biological samples were measured. Unexposed (blanks) and exposed samples were analyzed to determine the limits of detection and quantification of Pd (0.41 ± 0.01 ng/g for organisms, 860 ± 7.2 ng/L for water samples and 26 ± 1.7 ng/g for sediment samples). Non-spiked controls were placed together with the spiked treatments to account for possible cross-contamination during the assay. The total mean Pd amount recovered from each beaker ($N = 32$) after the assay corresponded to > 99 % of the spiked Pd, indicating a good mass balance across the experiment. Moreover, the contribution of unreacted organic compounds coming from the synthesis of PS-NPLs (e. g. released oligomers, organic surfactants or unreacted monomers) that may have affected the observed toxicological response was assessed by filtering the NPLs stock suspension through a 50 kDa MWCO ultrafiltration tubes and exposing the organisms to the same dose as the NPLs exposure. No toxicity was observed for *Anabaena* to these filtrates (Fig. S5).

2.5. Principal component analysis of environmental fate assays

To determine the influence of different factors that may affect the environmental fate assay, a principal component analysis (PCA) was conducted. The PCA was performed in RStudio software (Version 1.4.1717) where the function “prcomp” was applied with the scaled data to obtain the principal components (PC). Only PCs with an eigenvalue > 1 were considered for the selection of the most important indicators. The parameters used for the analysis at each compartment were: (i) pH, conductivity, ζ -potential, particle size distribution, TOC, surviving *D. magna* and PS-NPLs concentration for waters; (ii) moisture, chlorophyll *a* and PS-NPLs concentration for sediments; and (iii) chlorophyll *a* and PS-NPLs concentration for filters. The two PCs contributing to higher fraction explained variance were selected for the representation, all factors can be found in Table S5.

2.6. Data analysis

Results from at least three independent experiments were analyzed by calculating mean and standard deviation values for each treatment. Significant differences were evaluated through an overall one-way analysis of variance test (ANOVA) using SigmaPlot 11.0. Results were considered statistically significant when $p < 0.05$. When significant differences were observed, means and standard deviation (SD) between treatments and controls were compared using Dunnett's Method.

3. Results and discussion

3.1. PS-NPLs toxicity

Dose response curves for growth inhibition (*Anabaena* and

C. reinhardtii) and immobilization rate (*D. magna*) after exposure to increasing concentrations of PS-NPLs were determined by selecting the model that best fit the experimental data (Fig. S6). From these, the effective concentrations EC_{10} , EC_{50} , and EC_{80} were calculated (Table 1). 72hEC values for both photosynthetic organisms studied here were within the same order of magnitude; however, *Anabaena* showed lower 72hEC₅₀ and 72hEC₈₀ values than *C. reinhardtii* indicating that the cyanobacterium was more sensitive than the green alga. Similar differences have been previously found for the same organisms exposed to PS-NPLs [29,62,66,72,73] in agreement with a higher sensitivity of cyanobacteria than green algae to NPLs.

The 48hEC₅₀ and 48hEC₈₀ for the primary consumer, *D. magna*, were lower than those for the photosynthetic organisms, demonstrating a higher sensitivity of *D. magna* to PS-NPLs. The higher sensitivity of a primary consumer in comparison with algae has been also reported by Venâncio et al. [65] using PMMA-NPLs. The 48 hEC₅₀ found in the current study was similar to that reported for *D. magna* and *D. pulex* exposed to 30–70 nm PS-NPLs [33,66]. Regarding the toxicity of PS-NPLs with similar size to the ones used here, Pikuda et al. [44] reported a 48 hEC₅₀ value of 30.4 mg/L for *D. magna* exposed to 200 nm fluorescent PS-NPLs. The authors of this study attributed some toxicity to the preservatives used in commercial PS latexes in contrast to the finding of our work, in which no toxicity was observed from particle-free filtrate (Fig. S5). Considering NPLs of larger sizes, similar toxicities have been obtained by others in the literature. The reported EC₅₀ for *D. magna* exposed to 1 μ m polyethylene particles was 57.43 mg/L [51], suggesting that the observed mortality of NPLs may be related to physical damages derived from the attachment of particles onto the body of the organism. This has also been described elsewhere for small plastic particles in the micron size range and below [10]. There is also a previous work by Fringer et al. [17] on the impact of these nanoplastics to the bacterium *Shewanella oneidensis* where they found that these nano-PS had minimal impacts to bacterial viability but affected *S. oneidensis* in a way that can be related to the nano-PS attached or in proximity to the bacterium.

Overall, the concentrations at which the toxicity on algal growth or *D. magna* immobilization were observed were considerably higher than those expected to be found in the environment. Accordingly, it is important to assess the effect of NPLs using more sensitive endpoints in order to avoid overlooking potential sublethal effects that may impair organisms in the long term.

3.1.1. Analysis of mechanisms of toxic action

To study the mechanism of toxic action of PS-NPLs, exposure experiments were conducted at two different concentrations based on their low (close to the EC_{10}) and sublethal effect (close to the EC_{50}) on the cell growth of cyanobacterium and green alga (10 and 200 mg/L) and on the immobilization rate of *D. magna* neonates (10 and 80 mg/L). As shown in Fig. 2A and B, no effects on ROS levels were observed at the lowest concentrations tested on the photosynthetic organisms. However, *Anabaena* exposed to 200 mg/L showed a significant increase of general ROS, hydrogen peroxide and superoxide ions with values 300 %, 154 % and 213 % higher than controls, respectively. ROS overproduction was less pronounced in *C. reinhardtii* than in *Anabaena* since only a significant increase of superoxide ion formation was observed at the higher concentration. The results showed that general ROS levels significantly

Table 1

Effective concentrations of the PS-NPLs that caused 10 %, 50 % and 80 % of growth inhibition after 72 h (*Anabaena* and *C. reinhardtii*) and immobilization (*D. magna*) after 48 h of exposure calculated from the dose response curves \pm Standard Deviation. The model used for fitting the data is included in Fig. S6.

Effective concentration (mg/L)	<i>Anabaena</i>	<i>C. reinhardtii</i>	<i>D. magna</i>
EC ₁₀	18.9 \pm 12.3	14.6 \pm 6.1	14.5 \pm 5.1
EC ₅₀	151.3 \pm 22.5	247.8 \pm 32.7	48.7 \pm 5.7
EC ₈₀	383.8 \pm 66.5	878 \pm 157	83.7 \pm 8.4

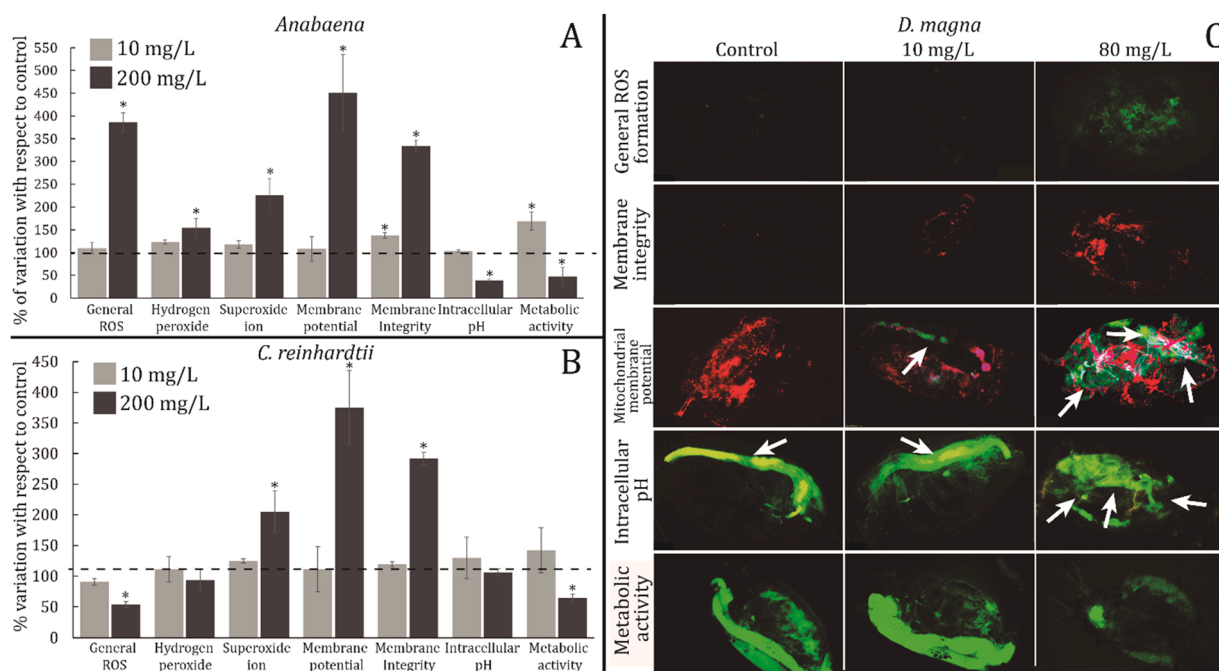


Fig. 2. Physiological alterations on *Anabaena* (A) and *C. reinhardtii* (B) after 72 h of exposure to 10 and 200 mg/L of PS-NPLs. Fluorimetry results are shown as the percentage of variation \pm SD with respect to the control (the results in raw fluorescence arbitrary units is shown in Fig. S7). Asterisks indicate treatments that are significantly different from the control (Dunnnett's test, $p < 0.05$). Representative images of the alterations observed by fluorescence microscopy on *D. magna* (C) after 48 h of exposure to 10 and 80 mg/L of PS-NPLs. Arrows point to the gut in the control and 10 mg/L treatments, and to damages to *D. magna* body in the 80 mg/L treatment. F.

decreased up to 53 % in *C. reinhardtii* exposed to 200 mg/L of NPLs, possibly due to an induction of ROS-scavenging enzymes. This defensive and adaptive response of cells to stressors that involve the activation of the machinery related to fight the oxidative imbalance has also been reported for *Halomonas alkaliphila* exposed to 20 mg/L of PS-NPLs [60]. Oxidative stress upon interaction of cells with NPLs has been previously observed for other aquatic photosynthetic organisms [16,20,31,65,66].

When ROS imbalance occurs, the high reactivity of ROS may damage the intracellular structures as well as cell membrane [13]. In this regard, at the lowest concentration tested here (10 mg/L) there was no alteration in membrane potential, but a slight loss of membrane integrity was observed only in *Anabaena*. However, at 200 mg/L, both *Anabaena* and *C. reinhardtii* displayed a strong increase (> 350 %) in fluorescence when treated with the fluorochrome DiBAC4(3), revealing a clear depolarization along with loss of membrane integrity (> 250 % increase in fluorescence for both organisms when treated with fluorochrome IP). Similar membrane damages attributed to physical interaction with NPLs have been previously reported for PS-NPLs as well as for (inorganic) engineered nanoparticles towards the cyanobacteria *Synechococcus elongatus* and *Anabaena* [15,47,62]. In the case of *Anabaena*, membrane damage was coupled with intracellular acidification, an effect that has been previously linked to a loss of membrane integrity or deficient proton pump activity [15,61]. Metabolic activity in *Anabaena* exposed to 10 mg/L showed a slight increase probably due to a hormetic response, whilst at 200 mg/L, an evident decrease was observed in both organisms.

Concerning *D. magna* (Fig. 2C), ROS overproduction was observed at 80 mg/L throughout the body but was not evident at lower exposure concentrations. Liu et al. [34] observed ROS overproduction in *D. pulex* for PS-NPLs for concentration as low as ≤ 2 mg/L, likely due to the lower particle size used (75 nm). ROS overproduction and cytoplasmic membrane damages have been previously described in *D. magna* exposed to organic hyperbranched nanoparticles and to secondary PHB-NPLs [19,37]. In this work, for the lowest concentration tested, *D. magna* showed evident alterations in cellular membrane integrity that

was clearly detected at 80 mg/L. Furthermore, a small increase in mitochondrial membrane depolarization in the gut was observed at 10 mg/L exposure concentrations, while at 80 mg/L the damage appeared to spread throughout the *D. magna* body (Fig. 2C). These alterations might be related to physical impairment caused by NPLs either in the digestive tract or in other organs. Cui et al. [11] reported the accumulation of PS-NPLs (52 nm) in the digestive tract of *D. galathea* as well as their translocation to different organs and linked the results to a decrease in survival and other toxic processes. In the same way, the acidification observed at the high concentration (80 mg/L) was not only located in the digestive tract (as it happened in controls, probably due to the probe being hydrolyzed by the hydrolytic enzymes present in the gut lumen, and in specimens exposed to 10 mg/L of PS-NPLs), but was widely distributed throughout Daphnia body, as shown in Fig. 2C, suggesting the uptake of the fluorescent probe by cells where the acetoxymethyl ester bound to BCECF is hydrolyzed releasing free BCECF that fluoresces inside the cells indicating intracellular acidification. Similar results were previously reported for *D. magna* exposed to secondary PHB-NPLs [19]. Cytoplasmic pH in eukaryotic cells is strictly regulated by the high buffering capacity of the cytosol plus ion transport mechanisms such as Na^+/H^+ antiporters. Thus, pH oscillations seem to be important in controlling the cell cycle and the proliferative capacity of cells [35]. Several researchers have found that intracellular pH is altered (either acidified or alkalinized) when cells are exposed to a range of contaminants/toxicants such as omeprazole [56], paraquat [46], UV-filters BP-3 and BP-4 [14] or Triclosan [18]. The fact that nanoparticles as the ones studied here also induce an alteration of intracellular pH in the tested organisms indicate that this parameter should be tested as the maintaining of the physiological pH in optimal range is important for the activity of many enzymes, for the efficiency of contractile elements and the conductivity of ion channels [35]. Redondo-Hasselerharm et al., [50], using the same PS-NPLs used in the present study, did not find statistically significant effects on the survival or growth of the secondary consumer *Gammarus pulex*. This may be related to interspecies variability effects, since *D. magna* has been reported to ingest up to

60 times more MPs than *G. pulex* [54]. This characteristic might influence the toxicity observed with NPLs, but it is worth noting that results from different size classes may not be transferable. Finally, we observed a decrease in metabolic activity for *D. magna* exposed to 80 mg/L. The alteration in metabolic activity was observed all throughout the *D. magna* body supporting the hypothesis that the damages triggered by PS-NPLs were not limited to the digestive tract.

In order to study the physical interactions between the PS-NPLs and the three organisms and their potential internalization, TEM-EDX was used. Pd-doped PS-NPLs in cell samples were detected by using the EDX detector (Fig. S8). As shown in Fig. 3, physical interactions between PS-NPLs and the three organisms were clearly observed at the higher concentrations tested (200 mg/L for the photosynthetic organisms and 80 mg/L for *D. magna*). In *Anabaena*, the direct interaction between PS-NPLs and the cellular envelope triggered cell damage and induced membrane disruption and distortions (Fig. 3A–C, red circles). Similarly, clear membrane alterations were also observed in *C. reinhardtii* at 200 mg/L (Fig. 3D–F). In both instances, these findings are likely related to the loss in membrane integrity that may be the consequence of PS-NPLs attachment to the cell surface. Particles in suspension may also block the access of light to photosynthetic organisms causing the so-called shading effect [23]. Although this effect is noteworthy when there is a strong aggregation of nanoparticles as the reported physiological alterations of the shading effects in algal cells exposed to superparamagnetic iron oxide nanoparticles [23]; given the high degree of interaction and observed adverse effects between the NPLs and the algal and cyanobacterial envelopes (Fig. 3), the contribution of the shading effect here is probably negligible. No clear NPL internalization was observed in any of the photosynthetic organisms.

Regarding *D. magna*, PS-NPLs deposited over the carapace surface forming aggregates attached to the chitin that covered the entire organism (Fig. 3K). This attachment of particles could hamper their mobility and long-term viability (Fig. 3G and H). In this regard, Cole et al., [10] reported that small plastic particles could be trapped between the external appendages and carapace segments of live copepods jeopardizing their viability. Moreover, particles compatible with the size and shape of the PS-NPLs were also observed within the digestive tract of *D. magna* (Fig. 3I). The internalization and dissemination in different organs of 52 nm PS-NPLs have been reported affecting the lipid storage in *D. galathea* [11]. Specifically, in *D. magna*, NPLs internalization has been clearly described for PMMA-NPLs (86–125 nm), for PS-NPLs (78–122 nm) and for fluorescent and metal-doped PS-NPLs (80–110 nm) [4,52,67]. Here, we could not unambiguously observe internalization of PS-NPLs beyond their presence in the digestive tract, however, based on the other physiological alterations observed throughout the study such as ROS overproduction that affects cytoplasmic membrane integrity and loss of cell viability (see Fig. 2C), the possibility of PS-NPLs internalization cannot be disregarded. Moreover, a portion of particles present in the digestive tract may be excreted with the fecal pellets as described for other NPLs and nanoparticles [2,37].

3.2. Environmental fate assays: microcosms studies

3.2.1. Static assays

The aim of this assay was to study the short-term distribution PS-NPLs in models of freshwater environments, by using natural water and sediments from a lake (for the static assay) and a river (for the stirring assay). Natural waters were spiked with 6 mg/L ($\sim 4.8 \times 10^8$ particles/mL) of PS-NPLs which corresponded to a concentration at which growth or immobilization effects were not observed in the organisms during the toxicological assay (*C. reinhardtii* and *D. magna*; Fig. 1). The differences between the two conditions were the water chemistry and sediment composition (lake versus river) and the fact that the assay was carried out under static or stirring conditions for the lake and river matrices, respectively (Fig. 1). After 48 h, the concentration of PS-NPLs was determined and their distribution in the four

compartments (Fig. S3) was assessed as follows: (i) NPLs dispersed or in aggregated with particulate material less than 1 μm suspended in the water column (cWC), (ii) NPLs associated with particulate material higher than 1 μm suspended in the water column (ncWC), (iii) NPLs adhered to the sediments (SC), and (iv) material adsorbed to or within *D. magna* (DC).

In the static assay and in the absence of organisms (Fig. 4A), most of the NPLs remained in the water column after 48 h either in the cWC (48.8 %) or in the ncWC (44.3 %) compartments. The NPLs in this compartment may be present in the form of heteroaggregates, but assessing heteroaggregation was beyond the scope of this study. The formation of heteroaggregates or microgels between NPLs and organic matter has been reported elsewhere [58], and NPLs settling could depend on water chemistry and/or their interaction with other natural water components [59]. Notably, nearly half of the particles (48.8 %) remained in the cWC compartment, ($< 1 \mu\text{m}$) so they might remain bioavailable as colloidal suspensions (either as individual particles or as aggregates). Approximately 7 % of the particles were in the SC after 48 h.

In comparison with the results when the organisms were not added, the presence of them increased the settling in all cases (Fig. 4B–D), likely due to the interactions between the NPLs and extracellular polymeric substances [26]. Additionally, the filter feeding behavior of *D. magna* might have increased the NPLs deposited via particles excreted with fecal pellets as previously reported for other particles [37,43]. The presence of *D. magna* also increased PS-NPLs content in the cWC compartment (Fig. 4B and D), and thus consequently fewer PS-NPLs were measured in the ncWC compartment. This implies that *D. magna* modified the aggregation of particles (leading to aggregates $< 1 \mu\text{m}$, either by homoaggregation or heteroaggregation), thereby altering the fate of PS-NPLs. Under static microcosm conditions, He et al. [20] reported that after 48 h half of the Pd-doped NPLs remained in the water column, while the other half were found in the sediments. In our case, under static conditions, most of the particles remained in the water column (approximately 90% considering both colloidal and non-colloidal particles/aggregates). However, it was not possible in either our study or in He et al. [20] to differentiate between particulate material in the proximity of the sediment or distributed in the water column. Therefore, if we consider the NPLs in the ncWC compartment as part of the sediment compartment, there would be approximately 50 % of NPLs in the water and 50 % in the sediment, in agreement with the results reported by He et al. [20].

No differences were found among the concentrations of ingested particles per daphnid, ranging from 0.10 ± 0.04 – 0.14 ± 0.06 ($\mu\text{g}/\text{organism}$) in the static assay (7800–10,920 particles/organism). These results were in agreement with Rist et al. [53], who reported an average value of $0.17 \mu\text{g}/\text{organism}$ in *D. magna* exposed to 100 nm PS-NPLs. Despite the presence of PS-NPLs, this body burden did not affect the survival of the organisms (Fig. S9).

3.2.2. Stirring assays

In comparison with the static assay, the concentration of PS-NPLs in the SC compartment was higher for all treatments. This effect may be related to an increase in particle collision (homoaggregation and heteroaggregation) due to stirring in combination with resuspension of the sediment by water turbulence leading to a higher interaction between the sediment material and the NPLs [30,7]. As in the static assay, NPLs in the SC compartment increased up to ~ 160 % in the presence of *C. reinhardtii* and *D. magna* (Fig. 4, panels F and G). In particular, in the assay using only *C. reinhardtii* (Fig. 4G), a strong decrease in the concentration of NPLs in the cWC compartment was observed which ended up directly into the sediments, since their concentration in the ncWC compartment was not altered. This could be related to a co-settling process between cells and NPLs, as suggested by Koelmans et al., [28], probably enhanced by the stirring conditions of this assay. In contrast, treatments containing *D. magna* followed the same trend as the static

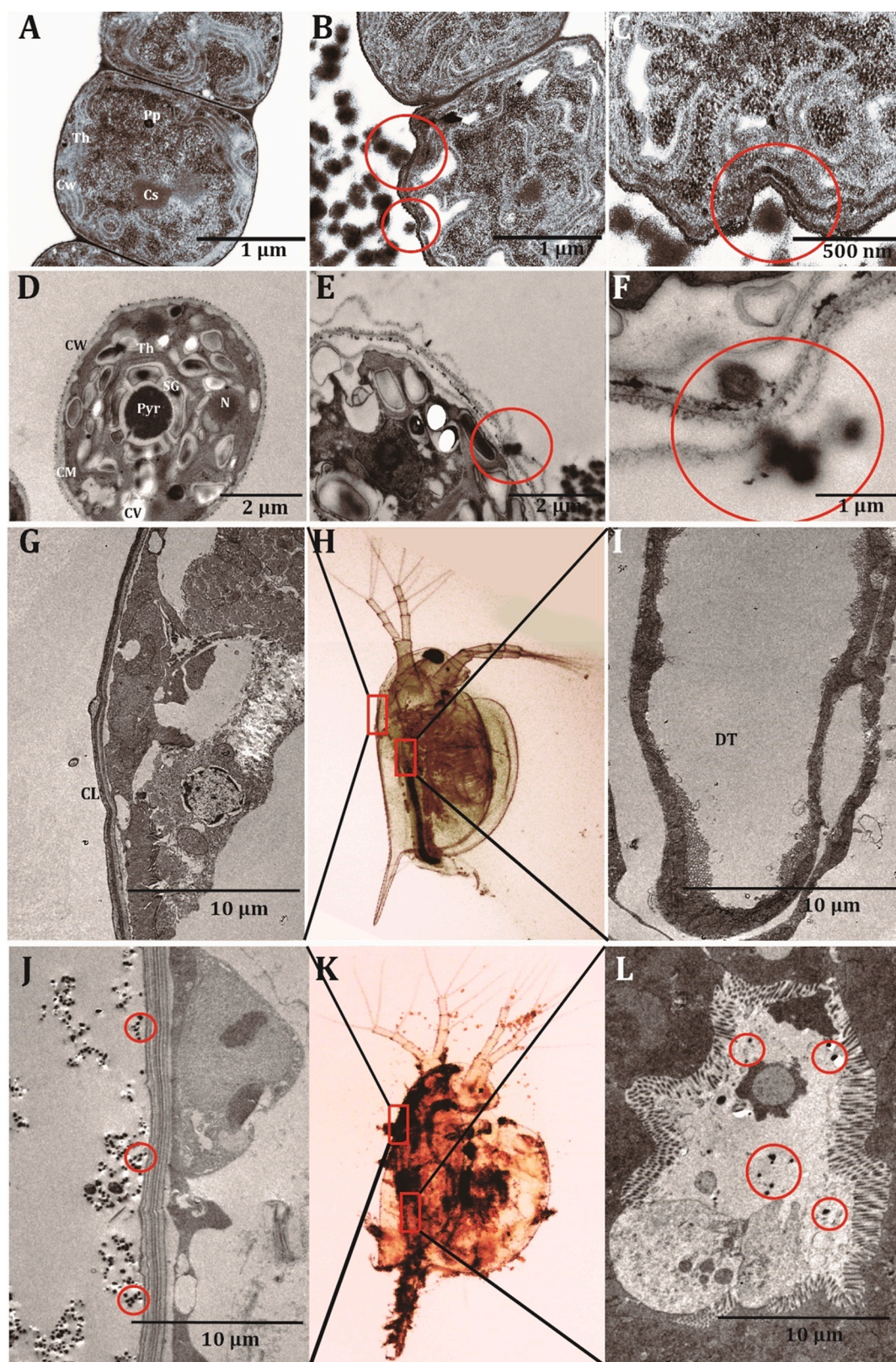


Fig. 3. TEM images of *Anabaena* (control, A, and treatment, B and C) and *C. reinhardtii* (control, D, and treatment, E and F) exposed for 72 h to 200 mg/L of PS-NPLs and *D. magna* (control, G–I, and treatments, J–L) exposed for 48 h to 80 mg/L of PS-NPLs (H and K are optical images of *D. magna* approximately indicating the location of TEM images). Red circles indicate the location of PS-NPLs interacting with the organisms. The energy dispersive x-ray spectra of NPLs interacting with the three model organisms can be found in Fig. S8. Acronyms: A) Cw: cell wall; Th: thylakoid membranes; Pp: polyphosphate granules; Cs: carboxysomes; D) CW: cell wall; CM: cell membrane; Th: thylakoid membranes; Pyr: pyrenoid; N: nucleus; SG: starch grains; CV: contractile vacuole; D) CL: chitin layer; I) DT: digestive tract.

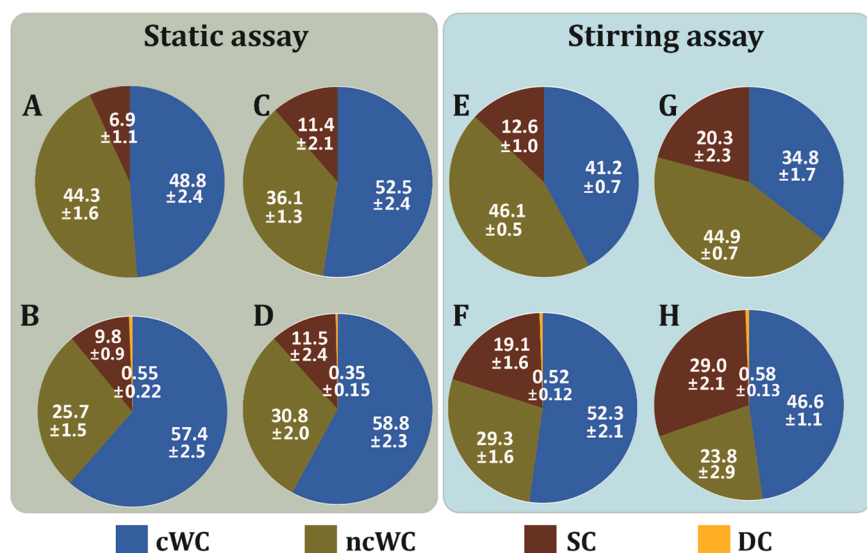


Fig. 4. Freshwater exposures under static (A–D) or stirring (E–H) across the exposures, including PS-NPLs alone (A and E), *C. reinhardtii* + PS-NPLs (C and G), *D. magna* + PS-NPLs (B and F), *C. reinhardtii* + *D. magna* + PS-NPLs (D and H). Proportions of PS-NPLs in each environmental compartment after 48 h at $23 \pm 2^\circ\text{C}$. NPLs content (as measured by Pd) was analyzed in four compartments: 1) freely dispersed or associated with natural particulate material $< 1 \mu\text{m}$ suspended in the water column (cWC), 2) associated with particulate material $> 1 \mu\text{m}$ in the water column (ncWC), 3) in the sediments (SC) and 4) adsorbed or internalized within *D. magna* (DC). Each pie plot represents the outcome from triplicates of one treatment (four independent experiments \pm SE).

assay, where there was a decrease of NPLs in the ncWC compartment and an increase in settled NPLs in the SC compartment. However, the presence of both organisms at the same time strongly increased the amount of settled NPLs by 230 % (Fig. 4H). These results support the hypothesis that NPLs transfer from the water column to the sediment led by consumers when food is available (*C. reinhardtii*), probably through the fecal pellets [37,43]. Accordingly, the overall lower chlorophyll *a* content under stirring conditions could mean that *D. magna* would be able to ingest higher amounts of *C. reinhardtii* than in static conditions,

resulting in increased water column to sediment transfer of NPLs (Fig. S10). As in the stirring assay, no differences were found among the ingested NPLs per daphnid, which showed body burdens of 0.15 ± 0.03 to 0.16 ± 0.04 ($\mu\text{g}/\text{organism}$), namely, 11,700–12,480 particles/organism, including all treatments (with and without the presence of *C. reinhardtii*).

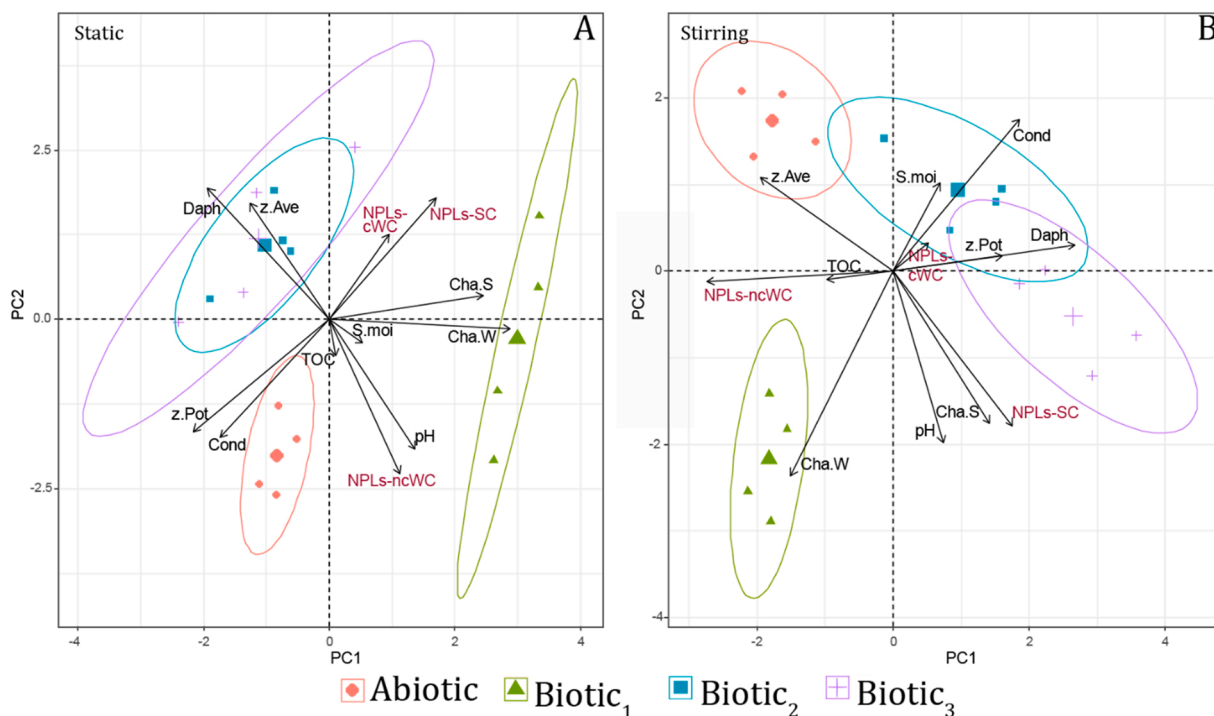


Fig. 5. Principal component analysis for static (A) and stirring (B) conditions. “x” and “y” axes correspond to the principal components one and two (PC 1 and PC2, respectively), which explain 53 % and 56 % of the variance observed between the two test conditions. The variation explained by the other two principal components with eigenvalues > 1 are shown in Table S5. The variables used are: pH, conductivity (Cond), ζ-potential (z.Pot), total organic carbon (TOC), DLS z-average (z.Ave), sediment moisture content in percentage (S.moi), chlorophyll *a* content in water and in sediment (Cha. W and Cha. S, respectively) and the number of live *D. magna* (Daph). In red, the variables corresponding to PS-NPLs content in cWC, ncWC and SC. Data are grouped by treatment: Abiotic (water + sediment + PS-NPLs); Biotic₁ (water + sediment + *C. reinhardtii* + PS-NPLs); Biotic₂ (water + sediment + *D. magna* + PS-NPLs); Biotic₃ (water + sediment + *C. reinhardtii* + *D. magna* + PS-NPLs).

3.3. Analysis of important variables controlling NPs fate in freshwater systems

In both static and stirring systems, most of the changes in NPLs distribution under different conditions led to a reduction of the amount of NPLs in the ncWC compartment, highlighting the role of heteroaggregates as an intermediate step during the distribution of NPLs in freshwater ecosystems. Given that the presence/absence of different types of organisms altered the physicochemical properties of the water column and, consequently, modified the stability of the NPLs, the potential factors responsible for PS-NPLs distribution were further assessed using PCA analyses. 12 variables were considered, which included physicochemical as well as biological parameters (Table S6). A two-dimensional plot for PCs for both static and stirring conditions were created (Fig. 5), which were able to account for > 50 % of the variance observed between the assays (Fig. S11).

PCA results for the static assay (Fig. 5A) showed that PS-NPLs in the ncWC compartment were grouped together with the pH and both were negatively correlated with *D. magna* and the size of all particulate material (variable denoted as *z-Ave*, which includes NPLs and other natural particles and heteroaggregates). The latter correlation suggests that NPLs in the ncWC compartment are being removed from this compartment due to changes in aggregate size and subsequent settling. However, *D. magna* could be also involved in this process. It is shown that, while feeding, this organism prefers larger particles instead of the smaller ones [53], therefore, *D. magna* could be mainly ingesting the larger particulate material, including NPLs heteroaggregates, reducing the amount of NPLs in the ncWC compartment. Regarding the influence of the primary producer, chlorophyll content in the sediment was positively correlated to NPLs concentrations in the SC compartment, supporting the hypothesis that an increase in settling may be the consequence of heteroaggregation processes between NPLs and algal cells, as hypothesized elsewhere [28].

NPLs in the cWC and SC compartments were closely related and negatively correlated to water conductivity and particle ζ -potential. These are crucial physicochemical parameters that affect the stability of NPLs [59], so the fate of NPLs in these two compartments are highly influenced by these factors. TOC content, an indicator of the NOM concentration, is better explained by the PC3 as shown in Fig. S12. This factor, along with pH, were the two water physicochemical parameters which best explained the distribution of NPLs in the abiotic compartments [32]. This highlights how the system and the correlation between factors change depending on the presence or absence of organisms.

Under the stirring conditions (Fig. 5B), the concentration of NPLs in the ncWC compartment was positively correlated to the size of all particulate material and, to a lesser extent, to the NOM content. This trend, which was also observed for the static system, supports the idea of the formation of heteroaggregates [58]. However, the size of the particulate material was negatively correlated to the presence of *D. magna*, highlighting their role in driving NPLs to the SC compartment possibly through fecal pellets, [4] as shown in PC3 (Fig. S12). NPLs in the cWC compartment appeared closely related to both particle ζ -potential and water NOM content (Fig. S12). The overall stability of the NPLs was thus higher with increasing ζ -potential values and NOM. This stabilization effect has been described for PS-NPLs due to the steric hindrance originated from the adsorbed macromolecular layer of different types of NOM [32,45]. Regarding NPLs in the SC compartment, this variable was closely correlated with the chlorophyll *a* content in sediments, in agreement with the hypothesis that the direct interaction between algal cells and PS-NPLs would induce their settling to the sediment (Fig. S10).

4. Conclusions

The toxicity of PS-NPLs was assessed towards three environmentally relevant organisms: two primary producers (one cyanobacterium and one green algae) which do not ingest NPLs and one primary consumer

(crustacean *Daphnia magna*) which is a particle-feeding organism. The fact that *D. magna* is able to ingest NPLs may explain the observed high toxicity of NPLs in this organisms as *Daphnia* showed the lowest 48 hEC₅₀ as compared to the 72 hEC₅₀ obtained for the primary producers. These results are in agreement with other studies regarding the toxicity of PS-NPLs, but here we have developed dose-response curves, which are generally scarcer in the literature. These curves can be used for addressing combined exposure with other pollutants as well as for in silico analysis such as QSAR models. Regarding the mechanisms of toxicity of NPLs, our results showed clear alterations in ROS homeostasis, metabolism and membrane impairment in the three test organisms when exposed to sub-lethal concentrations near their respective EC₅₀ values. For lower concentrations (i.e., those closer to the EC₁₀ values), only cellular membrane damage in the cyanobacterium and the crustacean were observed, which were attributed to the physical interaction with the PS-NPLs. Because of the high particle number needed to trigger these biological effects, acute impacts are not expected at current NPLs environmental concentrations but long-term (chronic) effects cannot be ruled out and therefore this area needs more research.

The Pd-doped PS particles used in this study are good tools for evaluating the body burden in particle-ingesting organisms such as *Daphnia* as well as to track them in different environmental compartments. Thus, the short-term environmental distribution microcosm study of PS-NPLs showed that most NPLs remained in the water column after 48 h, but less than 50 % remained as a colloidal suspension while the rest was found as non-colloidal particulate material (> 1 μ m). In this regard, NPLs fate is closely linked with their heteroaggregation behavior which could also drive NPLs transfer to the sediments. The concentration of NPLs in sediments was clearly promoted by the presence of organisms and considerably varied between the static and stirring systems. Assessing variable impacts of the presence of organisms and dynamic exposure conditions is currently under studied in NPLs research, but we show that these experimental factors are important to consider as they ultimately and significantly influence the results as to how NPLs behave in the environment. Indeed, NPLs are expected to be found in many natural water bodies with different water chemistry and turbulence, and thus overarching statements of NPLs fate are difficult to make.

This study shows that NPLs distribute in different compartments of the aquatic system over the course of 48 h, and may be harmful to biota but only at high concentrations which are not likely environmentally relevant. The lack of accurate analytic techniques to identify and quantify NPLs in real environmental matrices is a major drawback facing the field of plastics pollution today. In this context, the use of metal-doped NPLs are a useful tool for laboratory and mesocosm studies that mimic different environmental conditions. This study can thus help to expand the current knowledge of the toxicological effects of NPLs in relevant organisms along the aquatic trophic food chain and contribute to better understand their distribution in the environmental compartments, including biota. Our findings regarding the interaction of the NPLs with a primary producer and consumer in a microcosm highlights the modifying power of biota to alter the colloidal behavior and fate of NPLs in freshwater environments. This effect will need to be taken into account in future studies and in the environmental risk assessment of NPLs.

CRedit authorship contribution statement

Miguel Tamayo-Belda: Conceptualization, Investigation, Methodology, Writing – original draft, Writing – review & editing. **Ana Villanueva Pérez-Olivares:** Conceptualization, Investigation, Methodology, Writing – original draft. **Gerardo Pulido-Reyes:** Conceptualization, Investigation, Methodology, Writing – original draft, Writing – review & editing. **Keila Martín-Betancor:** Conceptualization, Investigation, Methodology, Writing – original draft. **Miguel González-Pleiter:** Conceptualization, Funding acquisition, Methodology, Writing – original draft, Writing – review & editing. **Francisco Leganés:**

Conceptualization, Funding acquisition, Methodology, Supervision, Writing – original draft, Writing – review & editing. **Denise M. Mitrano:** Conceptualization, Funding acquisition, Methodology, Writing – original draft, Writing – review & editing. **Roberto Rosal:** Conceptualization, Funding acquisition, Methodology, Supervision, Writing – original draft, Writing – review & editing. **Francisca Fernández-Piñas:** Conceptualization, Funding acquisition, Methodology, Supervision, Writing – original draft, Writing – review & editing.

Declaration of Competing Interest

The authors declare that they have no known competing financial interests or personal relationships that could have appeared to influence the work reported in this paper.

Data Availability

Data will be made available on request.

Acknowledgements

The authors acknowledge the financial support provided by the Spanish Government (Ministerio de Ciencia e Innovación, MICIN): PID2020-113769RB-C21/22, PLEC2021-007693 (Funded by MCIN/AEI/10.13039/501100011033 and by the European Union “NextGenerationEU”/PRTR”), TED2021-131609B-C32/33 grants and the Thematic Network of Micro- and Nanoplastics in the Environment (RED2018-102345-T, EnviroPlaNet Network). MTB is the recipient of a FPU (FPU17/01789) pre-doctoral contract by the Spanish Ministerio de Universidades. D.M.M. was funded through the Swiss National Science Foundation (SNF), Grant nos. PZ00P2_168105 and PCEFP2_186856. The authors gratefully acknowledge the support of IESMAT during physicochemical characterization of the nanoplastics. The authors would like to thank the research facility Interdepartmental Investigation Service (SIDI) for the use of their infrastructures and the technical support.

Appendix A. Supporting information

Supplementary data associated with this article can be found in the online version at [doi:10.1016/j.jhazmat.2022.130625](https://doi.org/10.1016/j.jhazmat.2022.130625).

References

- [1] Ahmed, S., 2016. Original research paper biological science estimation of total chlorophyll and total carotenoid contents for strains of *Anabaena* and *Gloeocapsa* through spectrophotometer part time lecturer, Department of Botany, Dhing College, Dhing: Nagaon Assam KEYW. *Biol Sci* 70–71.
- [2] Bergami, E., Bocci, E., Vannuccini, M.L., Monopoli, M., Salvati, A., Dawson, K.A., et al., 2016. Nano-sized polystyrene affects feeding, behavior and physiology of brine shrimp *Artemia franciscana* larvae. *Ecotoxicol Environ Saf* 123, 18–25. <https://doi.org/10.1016/j.ecoenv.2015.09.021>.
- [3] Blanco, F., Davranche, M., Hadri, H., El, Grassl, B., Gigault, J., 2021. Nanoplastics identification in complex environmental matrices: strategies for polystyrene and polypropylene. *Environ Sci Technol* 55, 8753–8759. <https://doi.org/10.1021/acs.est.1c01351>.
- [4] Booth, A.M., Hansen, B.H., Frenzel, M., Johnsen, H., Altin, D., 2016. Uptake and toxicity of methylmethacrylate-based nanoplastic particles in aquatic organisms. *Environ Toxicol Chem* 35, 1641–1649. <https://doi.org/10.1002/etc.3076>.
- [5] Cai, H., Xu, E.G., Du, F., Li, R., Liu, J., Shi, H., 2021. Analysis of environmental nanoplastics: progress and challenges. *Chem Eng J* 410, 128208. <https://doi.org/10.1016/j.cej.2020.128208>.
- [6] Cao, J., Liao, Y., Yang, W., Jiang, X., Li, M., 2022. Enhanced microalgal toxicity due to polystyrene nanoplastics and cadmium co-exposure: from the perspective of physiological and metabolomic profiles. *J Hazard Mater* 427, 127937. <https://doi.org/10.1016/j.jhazmat.2021.127937>.
- [7] Choudhary, A., Khandelwal, N., Singh, N., Tiwari, E., Ganie, Z.A., Darbha, G.K., 2022. Nanoplastics interaction with feldspar and weathering originated secondary minerals (kaolinite and gibbsite) in the riverine environment. *Sci Total Environ* 818, 151831. <https://doi.org/10.1016/j.scitotenv.2021.151831>.
- [8] Cirés, S., Wörmer, L., Timón, J., Wiedner, C., Quesada, A., 2011. Cylindrospermopsin production and release by the potentially invasive cyanobacterium *Aphanizomenon ovalisporum* under temperature and light gradients. *Harmful Algae* 10, 668–675. <https://doi.org/10.1016/j.hal.2011.05.002>.
- [9] Clark, N.J., Khan, F.R., Mitrano, D.M., Boyle, D., Thompson, R.C., 2022. Demonstrating the translocation of nanoplastics across the fish intestine using palladium-doped polystyrene in a salmon gut-sac. *Environ Int* 159, 106994. <https://doi.org/10.1016/j.envint.2021.106994>.
- [10] Cole, M., Lindeque, P., Fileman, E., Halsband, C., Goodhead, R., Moger, J., et al., 2013. Microplastic ingestion by zooplankton. *Environ Sci Technol* 47, 6646–6655. <https://doi.org/10.1021/es400663f>.
- [11] Cui, R., Kim, S.W., An, Y., 2017. Polystyrene nanoplastics inhibit reproduction and induce abnormal embryonic development in the freshwater crustacean *Daphnia galeata*. *Sci Rep* 7, 1–10. <https://doi.org/10.1038/s41598-017-12299-2>.
- [12] El Hadri, H., Gigault, J., Maxit, B., Grassl, B., Reynaud, S., 2020. Nanoplastic from mechanically degraded primary and secondary microplastics for environmental assessments. *NanoImpact* 17, 100206. <https://doi.org/10.1016/j.impact.2019.100206>.
- [13] Esperanza, M., Cid, Á., Herrero, C., Rioboo, C., 2015. Acute effects of a prooxidant herbicide on the microalga *Chlamydomonas reinhardtii*: screening cytotoxicity and genotoxicity endpoints. *Aquat Toxicol* 165, 210–221. <https://doi.org/10.1016/j.aquatox.2015.06.004>.
- [14] Esperanza, M., Seoane, M., Rioboo, C., Herrero, C., Cid, A., 2019. Differential toxicity of the UV-filters BP-3 and BP-4 in *Chlamydomonas reinhardtii*: a flow cytometric approach. *Sci Total Environ* 669, 412–420. <https://doi.org/10.1016/j.scitotenv.2019.03.116>.
- [15] Feng, L.J., Li, J.W., Xu, E.G., Sun, X.D., Zhu, F.P., Ding, Z., et al., 2019. Short-term exposure to positively charged polystyrene nanoparticles causes oxidative stress and membrane destruction in cyanobacteria. *Environ Sci Nano* 6, 3072–3079. <https://doi.org/10.1039/c9en00807a>.
- [16] Frehland, S., Kaegi, R., Hufenus, R., Mitrano, D.M., 2020. Long-term assessment of nanoplastic particle and microplastic fiber flux through a pilot wastewater treatment plant using metal-doped plastics. *Water Res* 182, 115860. <https://doi.org/10.1016/j.watres.2020.115860>.
- [17] Fringer, V.S., Fawcett, L.P., Mitrano, D.M., Maurer-Jones, M.A., 2020. Impacts of nanoplastics on the viability and riboflavin secretion in the model bacteria *Shewanella oneidensis*. *Front Environ Sci* 8, 97. <https://doi.org/10.3389/fenvs.2020.00097>.
- [18] González-Pleiter, M., Rioboo, C., Reguera, M., Abreu, I., Leganes, F., Cid, A., et al., 2017. Calcium mediates the cellular response of *Chlamydomonas reinhardtii* to the emerging aquatic pollutant Triclosan. *Aquat Toxicol* 186, 50–66. <https://doi.org/10.1016/j.aquatox.2017.02.021>.
- [19] González-Pleiter, M., Tamayo-Belda, M., Pulido-Reyes, G., Amariei, G., Leganés, F., Rosal, R., et al., 2019. Secondary nanoplastics released from a biodegradable microplastic severely impact freshwater environments. *Environ Sci Nano* 6, 1382–1392. <https://doi.org/10.1039/c8en01427b>.
- [20] He, S., Chi, H.Y., Li, C., Gao, Y., Li, Z.C., Zhou, X.X., et al., 2022. Distribution, bioaccumulation, and trophic transfer of palladium-doped nanoplastics in a constructed freshwater ecosystem. *Environ Sci Nano* 9, 1353–1363. <https://doi.org/10.1039/d1en00940k>.
- [21] Hernandez, L.M., Youse, N., Tufenkji, N., 2017. Are there nanoplastics in your personal care products. *Environ Sci Technol* 4, 280–285. <https://doi.org/10.1021/acs.estlett.7b00187>.
- [22] Holzer, M., Mitrano, D.M., Carles, L., Wagner, B., Tlili, A., 2022. Important ecological processes are affected by the accumulation and trophic transfer of nanoplastics in a freshwater periphyton-grazer food chain. *Environ Sci Nano* 9, 2990–3003. <https://doi.org/10.1039/D2EN00101B>.
- [23] Hurtado-Gallego, J., Pulido-Reyes, G., González-Pleiter, M., Salas, G., Leganés, F., Rosal, R., et al., 2020. Toxicity of superparamagnetic iron oxide nanoparticles to the microalga *Chlamydomonas reinhardtii*. *Chemosphere* 238, 124562. <https://doi.org/10.1016/j.chemosphere.2019.124562>.
- [24] IUPAC, 1971. Manual of symbols and terminology for physicochemical quantities and units. *Int Union Pure Appl Chem Div Phys Chem* 31, 577–638. <https://doi.org/10.1351/pac197231040577>.
- [25] Jambeck, J., Geyer, R., Wilcox, C., Siegler, T.R., Perryman, M., Andrady, A., et al., 2015. Plastic waste inputs from land into the ocean. *Mar Pollut* 347, 768. <https://doi.org/10.1016/j.science.2016.03.052>.
- [26] Junaid, M., Wang, J., 2021. Interaction of nanoplastics with extracellular polymeric substances (EPS) in the aquatic environment: a special reference to eco-corona formation and associated impacts. *Water Res* 201, 117319. <https://doi.org/10.1016/j.watres.2021.117319>.
- [27] Keller, A.S., Jimenez-Martinez, J., Mitrano, D.M., 2020. Transport of nano- and microplastic through unsaturated porous media from sewage sludge application. *Environ Sci Technol* 54, 911–920. <https://doi.org/10.1021/acs.est.9b06483>.
- [28] Koelmans, A.A., Besseling, E., Shim, W.J., 2015. Nanoplastics in the aquatic environment. *Critical review. Mar Anthropol Litter* 325–341. <https://doi.org/10.1007/978-3-319-16510-3>.
- [29] Li, S., Wang, P., Zhang, C., Zhou, X., Yin, Z., Hu, T., et al., 2020. Influence of polystyrene microplastics on the growth, photosynthetic efficiency and aggregation of freshwater microalgae *Chlamydomonas reinhardtii*. *Sci Total Environ* 714, 136767. <https://doi.org/10.1016/j.scitotenv.2020.136767>.
- [30] Li, Y., Wang, X., Fu, W., Xia, X., Liu, C., Min, J., et al., 2019. Interactions between nano/micro plastics and suspended sediment in water: implications on aggregation and settling. *Water Res* 161, 486–495. <https://doi.org/10.1016/j.watres.2019.06.018>.
- [31] Lins, T.F., O'Brien, A.M., Zargartalebi, M., Sinton, D., 2022. Nanoplastic state and fate in aquatic environments: multiscale modeling. *Environ Sci Technol* 56, 4017–4028. <https://doi.org/10.1021/acs.est.1c03922>.

- [32] Liu, Y., Huang, Z., Zhou, J., Tang, J., Yang, C., Chen, C., et al., 2020. Influence of environmental and biological macromolecules on aggregation kinetics of nanoplastics in aquatic systems. *Water Res* 186, 116316. <https://doi.org/10.1016/j.watres.2020.116316>.
- [33] Liu, Z., Yu, P., Cai, M., Wu, D., Zhang, M., Huang, Y., 2019. Polystyrene nanoplastic exposure induces immobilization, reproduction, and stress defense in the freshwater cladoceran *Daphnia pulex*. *Chemosphere* 215, 74–81. <https://doi.org/10.1016/j.chemosphere.2018.09.176>.
- [34] Liu, Z., Huang, Y., Jiao, Y., Chen, Q., Wu, D., Yu, P., et al., 2020. Polystyrene nanoplastic induces ROS production and affects the MAPK-HIF-1/NFκB-mediated antioxidant system in *Daphnia pulex*. *Aquat Toxicol* 220, 105420. <https://doi.org/10.1016/j.aquatox.2020.105420>.
- [35] Madhus, I.H., 1988. Regulation of intracellular pH in eukaryotic cells. *Biochem J* 250, 1–8. <https://doi.org/10.1042/bj2500001>.
- [36] Mahu, E., Moore-Hanaway, J., Maurer, B., Welschmeyer, N., Coale, K.H., 2018. The bulk fluorescein diacetate assay (FDA) as a technique for evaluating biotic impacts of crude oil to coastal sediments. *Environ Earth Sci* 77, 1–10. <https://doi.org/10.1007/s12665-018-7945-x>.
- [37] Martín-de-Lucía, I., Leganés, F., Fernández-Piñas, F., Rosal, R., 2019. Hyperbranched polymeric nanomaterials impair the freshwater crustacean *Daphnia magna*. *Environ Pollut* 249, 581–588. <https://doi.org/10.1016/j.envpol.2019.03.078>.
- [38] Materić, D., Peacock, M., Dean, J., Futter, M., Maximov, T., Moldan, F., et al., 2022. Presence of nanoplastics in rural and remote surface waters. *Environ Res Lett* 17, 054036. <https://doi.org/10.1088/1748-9326/ac68f7>.
- [39] Mattsson, K., Jocić, S., Doverbratt, I., Hansson, L., 2018. Nanoplastics in the aquatic environment. In: *Microplastic contamination in aquatic environments*. Elsevier Inc., pp. 379–399. <https://doi.org/10.1016/B978-0-12-813747-5.00013-8>.
- [40] Mitrano, D.M., Beltzung, A., Frehland, S., Schmiedgruber, M., Cingolani, A., Schmidt, F., 2019. Synthesis of metal-doped nanoplastics and their utility to investigate fate and behaviour in complex environmental systems. *Nat Nanotechnol* 14, 362–368. <https://doi.org/10.1038/s41565-018-0360-3>.
- [41] OECD, 2011. Guidelines for the testing of chemicals, 201. Freshwater alga and cyanobacteria, growth inhibition test. *Organ Econ Co-Oper Dev* 4–7. <https://doi.org/10.1145/1294046.1294048>.
- [42] OECD, 2004. Guidelines for the testing of chemicals, 202. *Daphnia* sp., Acute Immobilisation Test. (<https://doi.org/10.1787/9789264069947-en>).
- [43] Pérez-Guevara, F., Roy, P.D., Kutralam-Muniasamy, G., Shruti, V.C., 2021. A central role for fecal matter in the transport of microplastics: an updated analysis of new findings and persisting questions. *J Hazard Mater Adv* 4, 100021. <https://doi.org/10.1016/j.hazadv.2021.100021>.
- [44] Pikuda, O., Xu, E.G., Berk, D., Tufenkji, N., 2019. Toxicity assessments of micro- and nanoplastics can be confounded by preservatives in commercial formulations. *Environ Sci Technol Lett* 6, 21–25. <https://doi.org/10.1021/acs.estlett.8b00614>.
- [45] Pradel, A., Ferreres, S., Veclin, C., El Hadri, H., Gautier, M., Grassl, B., et al., 2021. Stabilization of fragmental polystyrene nanoplastic by natural organic matter: insight into mechanisms. *ACS EST Water* 1, 1198–1208. <https://doi.org/10.1021/acsestwater.0c00283>.
- [46] Prado, R., Rioboo, C., Herrero, C., Cid, A., 2012. Screening acute cytotoxicity biomarkers using a microalga as test organism. *Ecotoxicol Environ Saf* 86, 219–226. <https://doi.org/10.1016/j.ecoenv.2012.09.015>.
- [47] Pulido-Reyes, G., Briffa, S.M., Hurtado-Gallego, J., Yudina, T., Leganés, F., Puentes, V., et al., 2019. Internalization and toxicological mechanisms of uncoated and PVP-coated cerium oxide nanoparticles in the freshwater alga *Chlamydomonas reinhardtii*. *Environ Sci Nano* 6, 1959–1972. <https://doi.org/10.1039/c9en00363k>.
- [48] Pulido-Reyes, G., Magherini, L., Bianco, C., Sethi, R., von Gunten, U., Kaegi, R., et al., 2022. Nanoplastic removal in drinking water by ozonation and filtration: laboratory-scale, pilot-scale and modeling studies. *SSRN Electron J* 1–42. <https://doi.org/10.2139/ssrn.4028212>.
- [49] del Real, A.E.P., Mitrano, D.M., Castillo-Michel, H., Wazne, M., Reyes-Herrera, J., Bortel, E., et al., 2022. Assessing implications of nanoplastics exposure to plants with advanced nanometrology techniques. *J Hazard Mater* 430, 128356. <https://doi.org/10.1016/j.jhazmat.2022.128356>.
- [50] Redondo-Hasselerharm, P.E., Vink, G., Mitrano, D.M., Koelmans, A.A., 2021. Metal-doping of nanoplastics enables accurate assessment of uptake and effects on *Gammarus pulex*. *Environ Sci Nano* 8, 1761–1770. <https://doi.org/10.1039/d1en00068c>.
- [51] Rehse, S., Kloas, W., Zarfl, C., 2016. Short-term exposure with high concentrations of pristine microplastic particles leads to immobilisation of *Daphnia magna*. *Chemosphere* 153, 91–99. <https://doi.org/10.1016/j.chemosphere.2016.02.133>.
- [52] Reynolds, A., 2019. Evaluation of non-invasive toxicological analysis of nanoplastics in relative in vivo conditions. *Environ Sci Nano* 6, 2832–2849. <https://doi.org/10.1039/c9en00434c>.
- [53] Rist, S., Baum, A., Hartmann, N.B., 2017. Ingestion of micro- and nanoplastics in *Daphnia magna* – quantification of body burdens and assessment of feeding rates and reproduction. *Environ Pollut* 228, 398–407. <https://doi.org/10.1016/j.envpol.2017.05.048>.
- [54] Scherer, C., Brennholt, N., Reifferscheid, G., Wagner, M., 2017. Feeding type and development drive the ingestion of microplastics by freshwater invertebrates. *Sci Rep* 7, 1–9. <https://doi.org/10.1038/s41598-017-17191-7>.
- [55] Sendra, M., Pereiro, P., Yeste, M.P., Mercado, L., Figueras, A., Novoa, B., 2021. Size matters: zebrafish (*Danio rerio*) as a model to study toxicity of nanoplastics from cells to the whole organism. *Environ Pollut* 268, 115769. <https://doi.org/10.1016/j.envpol.2020.115769>.
- [56] Seoane, M., Esperanza, M., Cid, Á., 2017. Cytotoxic effects of the proton pump inhibitor omeprazole on the non-target marine microalga *Tetraselmis suecica*. *Aquat Toxicol* 191, 62–72. <https://doi.org/10.1016/j.aquatox.2017.08.001>.
- [57] Shen, M., Zhang, Y., Zhu, Y., Song, B., Zeng, G., Hu, D., et al., 2019. Recent advances in toxicological research of nanoplastics in the environment: a review. *Environ Pollut* 252, 511–521. <https://doi.org/10.1016/j.envpol.2019.05.102>.
- [58] Shiu, R.F., Vazquez, C.I., Tsai, Y.Y., Torres, G.V., Chen, C.S., Santschi, P.H., et al., 2020. Nano-plastics induce aquatic particulate organic matter (microgels) formation. *Sci Total Environ* 706, 135681. <https://doi.org/10.1016/j.scitotenv.2019.135681>.
- [59] Singh, N., Tiwari, E., Khandelwal, N., Darbha, G.K., 2019. Understanding the stability of nanoplastics in aqueous environments: effect of ionic strength, temperature, dissolved organic matter, clay, and heavy metals. *Environ Sci Nano* 6, 2968–2976. <https://doi.org/10.1039/c9en00557a>.
- [60] Sun, X., Chen, B., Li, Q., Liu, N., Xia, B., Zhu, L., et al., 2018. Toxicities of polystyrene nano- and microplastics toward marine bacterium *Halomonas alkaliphila*. *Sci Total Environ* 642, 1378–1385. <https://doi.org/10.1016/j.scitotenv.2018.06.141>.
- [61] Tamayo-Belda, M., González-Pleiter, M., Pulido-Reyes, G., Martín-Betancor, K., Leganés, F., Rosal, R., et al., 2019. Mechanism of the toxic action of cationic G5 and G7 PAMAM dendrimers in the cyanobacterium. *Environ Sci Nano* 6, 863–878. <https://doi.org/10.1039/C8EN01409D>.
- [62] Tamayo-Belda, M., Vargas-Guerrero, J.J., Martín-Betancor, K., Pulido-Reyes, G., González-Pleiter, M., Leganés, F., et al., 2021. Understanding nanoplastic toxicity and their interaction with engineered cationic nanoplastics in microalgae by physiological and proteomic approaches. *Environ Sci Nano* 8, 2277–2296. <https://doi.org/10.1039/d1en00284h>.
- [63] Tamayo-Belda, M., Pulido-Reyes, G., González-Pleiter, M., Martín-Betancor, K., Leganés, F., Rosal, R., et al., 2022. Identification and toxicity towards aquatic primary producers of the smallest fractions released from hydrolytic degradation of polycaprolactone microplastics. *Chemosphere* 303, 134966. <https://doi.org/10.1016/j.chemosphere.2022.134966>.
- [64] Vélez-Escamilla, L.Y., Contreras-Torres, F.F., 2022. Latest advances and developments to detection of micro- and nanoplastics using surface-enhanced Raman spectroscopy. *Part Part Syst Charact* 39, 1–17. <https://doi.org/10.1002/ppsc.202100217>.
- [65] Venâncio, C., Ferreira, I., Martins, M.A., Soares, A.M.V.M., Lopes, I., Oliveira, M., 2019. The effects of nanoplastics on marine plankton: a case study with polymethylmethacrylate. *Ecotoxicol Environ Saf* 184, 109632. <https://doi.org/10.1016/j.ecoenv.2019.109632>.
- [66] Verdú, I., Amariei, G., Plaza-Bolaños, P., Agüera, A., Leganés, F., Rosal, R., et al., 2022. Polystyrene nanoplastics and wastewater displayed antagonistic toxic effects due to the sorption of wastewater micropollutants. *Sci Total Environ* 819, 153063. <https://doi.org/10.1016/j.scitotenv.2022.153063>.
- [67] Vicentini, D.S., Nogueira, D.J., Melegari, S.P., Arl, M., Köerich, J.S., Cruz, L., et al., 2019. Toxicological evaluation and quantification of ingested metal-core nanoplastic by *Daphnia magna* through fluorescence and inductively coupled plasma-mass spectrometric methods. *Environ Toxicol Chem* 38, 2101–2110. <https://doi.org/10.1002/etc.4528>.
- [68] Villacorta, A., Rubio, L., Alaraby, M., López-Mesas, M., Fuentes-cebrian, V., Moriones, O.H., et al., 2022. A new source of representative secondary PET nanoplastics. Obtention, characterization, and hazard evaluation. *J Hazard Mater* 439, 129593. <https://doi.org/10.1016/j.jhazmat.2022.129593>.
- [69] Wahl, A., Le Juge, C., Davranche, M., El Hadri, H., Grassl, B., Reynaud, S., et al., 2021. Nanoplastic occurrence in a soil amended with plastic debris. *Chemosphere* 262, 127784. <https://doi.org/10.1016/j.chemosphere.2020.127784>.
- [70] Weber, A., Schwiebs, A., Solhaug, H., Stenvik, J., Nilsen, A.M., Wagner, M., et al., 2022. Nanoplastics affect the inflammatory cytokine release by primary human monocytes and dendritic cells. *Environ Int* 163, 107173. <https://doi.org/10.1016/j.envint.2022.107173>.
- [71] Xu, Y., Ou, Q., Jiao, M., Liu, G., Hoek, J.P., Van Der, 2022. Identification and quantification of nanoplastics in surface water and groundwater by pyrolysis gas chromatography – mass spectrometry. *Environ Sci Technol* 56, 4988–4997. <https://doi.org/10.1021/acs.est.1c07377>.
- [72] Yang, W., Gao, P., Li, H., Huang, J., Zhang, Y., Ding, H., et al., 2021. Mechanism of the inhibition and detoxification effects of the interaction between nanoplastics and microalgae *Chlorella pyrenoidosa*. *Sci Total Environ* 783, 146919. <https://doi.org/10.1016/j.scitotenv.2021.146919>.
- [73] Zheng, X., Yuan, Y., Li, Y., Liu, X., Wang, X., Fan, Z., 2021. Polystyrene nanoplastics affect growth and microcystin production of *Microcystis aeruginosa*. *Environ Sci Pollut Res* 28, 13394–13403. <https://doi.org/10.1007/s11356-020-10388-w>.
- [74] Zhou, X.X., He, S., Gao, Y., Li, Z.C., Chi, H.Y., Li, C.J., et al., 2021. Protein corona-mediated extraction for quantitative analysis of nanoplastics in environmental waters by pyrolysis gas chromatography/mass spectrometry. *Anal Chem* 93, 6698–6705. <https://doi.org/10.1021/acs.analchem.1c00156>.